

Organic & Biomolecular Chemistry

Accepted Manuscript



This is an *Accepted Manuscript*, which has been through the Royal Society of Chemistry peer review process and has been accepted for publication.

Accepted Manuscripts are published online shortly after acceptance, before technical editing, formatting and proof reading. Using this free service, authors can make their results available to the community, in citable form, before we publish the edited article. We will replace this *Accepted Manuscript* with the edited and formatted *Advance Article* as soon as it is available.

You can find more information about *Accepted Manuscripts* in the [Information for Authors](#).

Please note that technical editing may introduce minor changes to the text and/or graphics, which may alter content. The journal's standard [Terms & Conditions](#) and the [Ethical guidelines](#) still apply. In no event shall the Royal Society of Chemistry be held responsible for any errors or omissions in this *Accepted Manuscript* or any consequences arising from the use of any information it contains.



Journal Name

ARTICLE

Synthesis and Electronic Properties of π -Extended Flavins

L.N. Mataranga-Popa,^{a,b} I. Torje,^b T. Ghosh,^a M. J. Leitl,^a A. Späth,^a M. L. Novianti,^c R. D. Webster^{c*} and B. König^{a*}

Received 00th January 20xx,
Accepted 00th January 20xx

DOI: 10.1039/x0xx00000x

www.rsc.org/

Flavin derivatives with an extended π -conjugation were synthesized in moderate to good yields from aryl bromides via a Buchwald-Hartwig palladium catalyzed amination protocol, followed by condensation of the corresponding aromatic amines with violuric acid. The electronic properties of the new compounds were determined by absorption and emission spectroscopy and cyclic voltammetry. The compounds absorb up to 550 nm and show strong luminescence. The photoluminescence quantum yields ϕ_{PL} measured in dichloromethane reach 80 % and in PMMA (poly(methyl methacrylate)) 77 %, respectively, at ambient temperature. The electrochemical redox behaviour of the π -extended flavins follows the mechanism previously described for the parent flavin.

Flavins are the prosthetic group of flavoproteins and universal redox cofactors in biology.¹⁻³ They play an important role in light, oxygen, and voltage-sensitive (LOV) domains sensitive for blue light excitation.⁴ However, flavins have also found many applications in photocatalysis⁵⁻¹¹ or as photosensitizers¹²⁻¹⁴ in singlet oxygen generation for synthesis or in photodynamic disinfection.^{13, 15, 16} The local environment,¹⁷ hydrogen bonding^{18, 19}, π - π stacking²⁰ or metal coordination^{21, 22} to the chromophore and the type and position of substituents²³ determine the redox potentials and the photo-physical properties of flavin derivatives. Donor-acceptor systems, in which flavins are covalently linked to other chromophores showing different absorption have been synthesized^{24, 25} and used in photo-voltaic devices,²⁶ molecular switching or molecular logic gates.^{26, 27} Oxidized forms of flavin derivatives act as electron acceptor in photoinduced electron transfer (PET)^{28, 29} and are known to bind different metal ions inducing a positive shift in their one-electron reduction potentials²⁹ and long-lived charge-separation.²⁹ A less explored option to modify the optical and electronic properties of flavins is the extension of their aromatic π -system. An extended conjugation length is expected to shift the absorption maxima to longer wavelength and affect the extinction coefficient and redox properties of the chromophore.^{30, 31} We report here the synthesis and electronic properties of three new flavins with

extended aromatic π -systems.

Results and discussion

Synthesis

The synthesis of new π -system extended flavins **3a**, **3b** and **3c**³² was accomplished by the condensation³³ of violuric acid **1** with the corresponding amines **2 a-c** as starting materials. The amines were obtained via Buchwald - Hartwig amination³⁴ in good to very good yields. The subsequent condensation of amines **2a – 2c** with violuric acid **1** in boiling acetic acid easily furnished multi-gram quantities of flavins **3 a-c** moderate to good yields (Scheme 1).

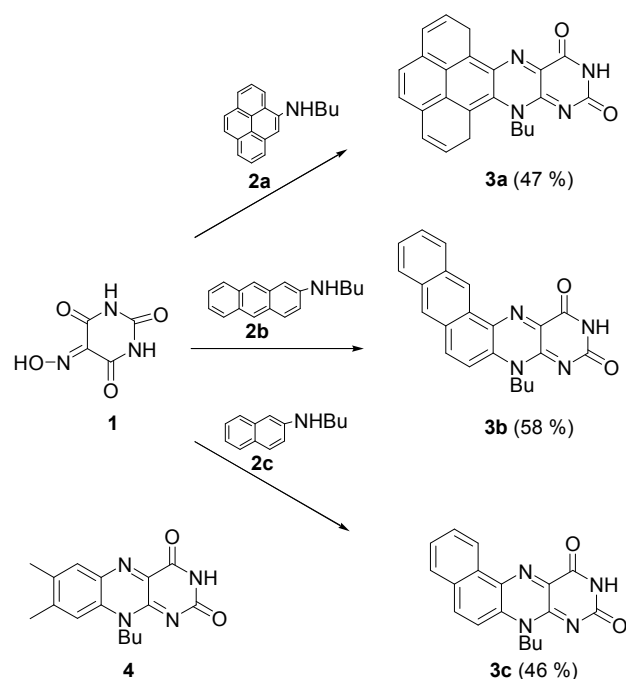
The structures of the flavins **3a – 3c** were determined by NMR spectroscopy and confirmed by high resolution mass spectrometry and elemental analysis. The electronic properties of the flavin derivatives **3a – 3c** were investigated by absorption and emission spectroscopy (Table 1) and cyclic voltammetry. Furthermore, the fluorescence quantum yields of the chromophores were determined with an integrating sphere accessory.

^a, University of Regensburg, Universitätsstraße 31, 93053 Regensburg, Germany.
E-mail: burkhard.koenig@chemie.uni-regensburg.de.

^b, Babes-Bolyai University Cluj-Napoca, Faculty of Chemistry and Chemical Engineering, Arany Janos Str. 11, Cluj-Napoca, 400428 Romania

^c Division of Chemistry & Biological Chemistry, School of Physical and Mathematical Sciences, Nanyang Technological University, 21 Nanyang Link, 637371 Singapore. E-mail: Webster@ntu.edu.sg.

† Electronic Supplementary Information (ESI) available: Detailed experimental procedures, copies of ¹H and ¹³C NMR spectra of compounds **2a–2c** and **3a–3c**; and selected molecular orbitals for compounds **3a–3c**. DOI: 10.1039/b000000x/



Scheme 1. Synthesis of the flavins **3a** – **3c**. Reaction conditions: amines **2a** – **2c** (1.2 eq.), violic acid **1** (1 eq.), acetic acid, reflux, 19 h. For comparison, the structure of the parent flavin **4** is shown.

Theoretical calculations

Computational investigations are particularly useful for understanding trends observed in the electrochemical and photophysical properties of molecular materials. Thus, density functional theory (DFT) and time dependent density functional (TDDF) calculations were performed to gain additional understanding of the electronic structure of the π -expanded flavins (**3a**, **3b**, and **3c**).

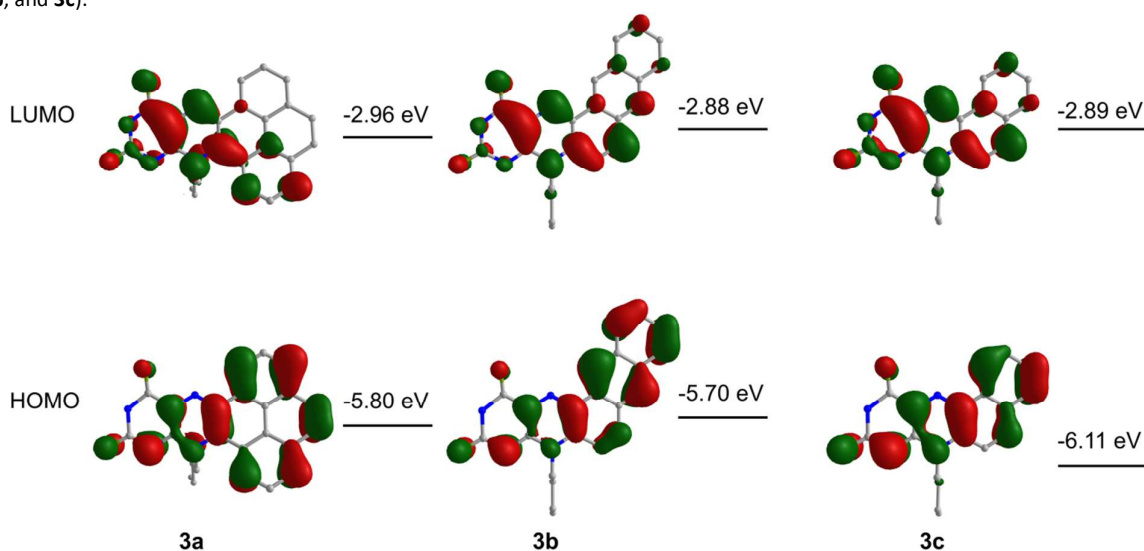


Figure 1. HOMOs and LUMOs of compounds **3a**, **3b**, and **3c**. The plots result from DFT calculations performed on the B3LYP/6-31G** level of theory. The iso-contour value was set to 0.03. Further molecular orbitals and the corresponding energies are displayed in the ESI.

Interestingly, the contour curves of the lowest unoccupied molecular orbitals (LUMOs) look similar for all three investigated compounds being largely unaffected by the π -extension (Figure 1). Also, the LUMO energies are similar ranging from -2.88 eV to -2.96 eV. In contrast to this, the highest occupied molecular orbitals (HOMOs) are delocalized over large parts of the molecule for all investigated compounds (Figure 1). Consequently, the HOMO energies vary in a wider energy range from -5.70 eV to -6.11 eV. TDDFT calculations revealed the transitions between these frontier orbitals determining the lowest excited single state S_1 . The corresponding transition energies amount to 2.47 eV (**3a**), 2.44 eV (**3b**), and 2.85 eV (**3c**). This is in agreement with the experimental results (see below) which show that the emission energies of compound **3a** and **3b** are similar, whereas the emission of compound **3c** is clearly blue-shifted. This trend is also seen in the absorption spectra.



Journal Name

ARTICLE

Electronic properties

The UV-visible absorption and emission spectral data of the flavins in two different organic solvents and in a polymer matrix (PMMA -poly(methyl methacrylate)) are summarized in Table 1. The absorption and emission spectra of the flavin derivatives **3a**, **3b**, **3c** and the butyl flavin derivative **4** recorded in DMSO are displayed in Figures 2a and 2b. All new derivatives show a complex absorption profile characteristic for the presence of multiple chromophores. The flavins exhibit intense absorption bands in the range of 306 – 543 nm. The $S_0 \rightarrow S_1$ band around 440 nm, characteristic for the parent flavin **4** is red shifted by 15 nm for compound **3c**, 52 nm for **3b** and 57 nm for **3a**, respectively, in DMSO solution, indicating a decreased HOMO – LUMO gap as expected with increasing π -conjugation. Furthermore, the absorption bands in the range 306 – 400 nm show a vibrational fine structure characteristic for the isolated naphthalene, anthracene and pyrene chromophore.³⁵ However, the molar extinction coefficient of the anthracene derivative **3b** is significantly higher than those observed for pyrene **3a** and naphthalene **3c**. A likely reason for this is the extended linear conjugated system.

Compounds **3a** and **3b** show an intense orange emission under daylight irradiation, while **3c** emits in the green.

The emission spectrum of **3c** shows a vibrational structure, similar to that of butyl flavin (**4**), with a spacing of 1000 cm^{-1} . This energy spacing corresponds to the characteristic stretching modes of isoalloxazines. Furthermore, the structured emission indicates that the emission is originating from a localized $\pi-\pi^*$ transition. In contrast, the emissions of **3a** and **3b** are broad and do not exhibit any structure indicating that the emission originates from a state with some charge transfer character. This assignment is also supported by the TD-DFT calculation (Figure 1), which predicts that the S_1 state is of partial charge transfer character for **3a** and **3b** due to HOMO orbitals delocalized over the entire molecule and LUMO orbitals localized on the isoalloxazine part. In addition, the emission maxima show a clear dependence on the polarity of the solvent, which is typical for charge transfer transitions. In the case of **3a**, in DCM (ET (30) = 41.1)³⁶ the emission peaks at 610 nm whereas it is red shifted by 18 nm in DMSO (ET (30) = 45.0)³⁶ to 628 nm. Compound **3b** exhibits a similar red shift of 20 nm from 585 nm to

605 nm when we go from DCM to DMSO. For flavin **3c** a corresponding shift from 511 nm to only 516 nm is observed.

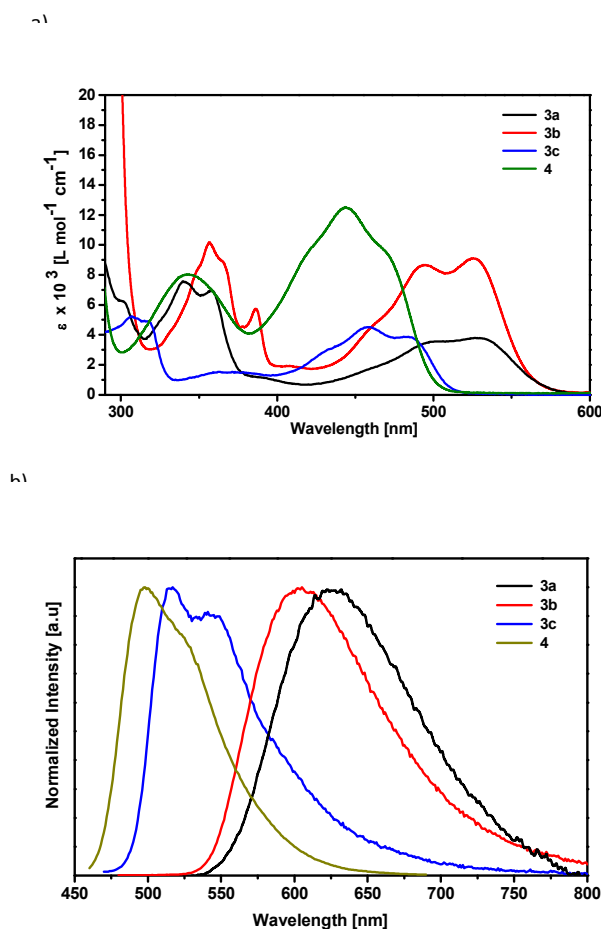


Figure 2. a) UV-Vis and b) emission spectra of 1.0×10^{-4} M solutions of **3a** (black line), **3b** (red line), **3c** (blue line) and **4** (green line) in DMSO at 300K ($\lambda_{\text{exc}} = 450 \text{ nm}$).

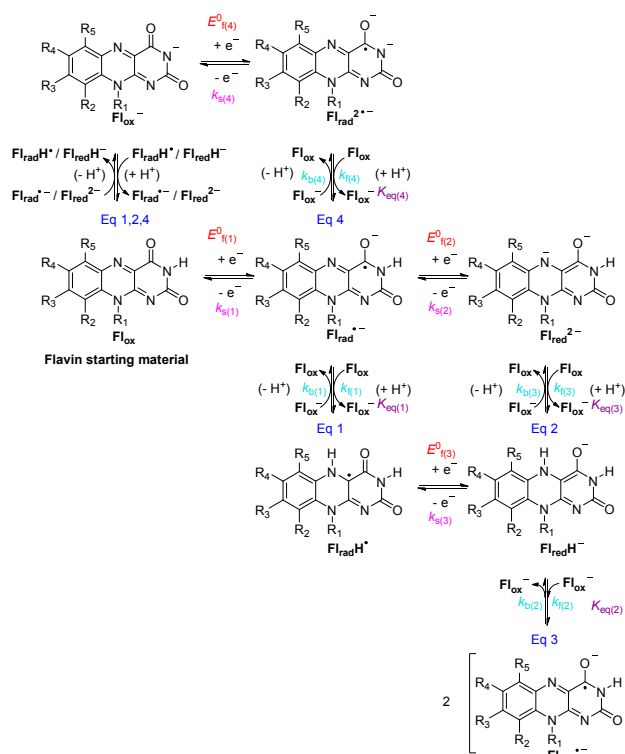
Table 1. Selected photophysical properties of the flavins **3a** – **3c** and **4** measured at ambient and liquid nitrogen temperature, respectively. $\lambda_{\text{abs.max}}$ is the peak wavelength of the absorption spectrum, $\lambda_{\text{em.max}}$ is the peak wavelength of the emission spectrum, τ the emission decay time, and Φ_{PL} the photoluminescence quantum yield. PMMA: poly(methyl methacrylate)

Compound	Solvent polymer	$\lambda_{\text{abs.max}}$ [nm]	$\lambda_{\text{em.max}}$ (300K) [nm]	τ (300K) / τ (77K) [ns]	Φ_{PL} (300K) / Φ_{PL} (77K) [%]
3a	DCM	339, 355, 503, 543	610		60 / 80
	DMSO	340, 357, 500, 530	628	9 / 15	46 / 57
	PMMA		580	11 / 11	50 / 74
3b	DCM	361, 384, 505, 542	585		24 / 70
	DMSO	357, 386, 495, 526	605	7 / 16	53 / 65
	PMMA		628	6 / 6	28 / 35
3c	DCM	306, 462 , 490	511, 544 (sh)		80 / \approx 100
	DMSO	306, 457 , 486	516, 545 (sh)	2 / 11	13 / 33
	PMMA		518 (sh), 539	11 / 11	77 / 80
4	DMSO	343, 443 , 470	498, 526 (sh)	-	14

The emission quantum yields of the new compounds **3a** – **3c** vary with solvent and temperature. In solution at $T = 300$ K the emission quantum yields are between 24 to 80 % in DCM, 13 to 53 % in DMSO and 13 to 77 % in PMMA. The corresponding Φ_{PL} values at nitrogen temperature increase, which may be explained by a decrease of non-radiative deactivations on cooling. The life times at 300K of the excited states of the three compounds are in the range of 2 to 9 ns in DMSO and 6 – 11 ns in PMMA. The values increase only slightly when decreasing the temperature from 300K to 77 K; in PMMA the same values are observed for both temperatures. We assume that the radiative emission at 300 K and 77 K originates from the singlet excited state without triplet state involvement.

Redox properties

The voltammetric behaviour and reduction mechanism of compounds **3a**, **3b** and **3c** in DMSO can be interpreted based on the mechanism for the closely related riboflavin, which has been studied in detail previously.³⁷⁻³⁹



Scheme 2. General electrochemical reduction mechanism for flavins in DMSO.

The variable scan rate cyclic voltammograms of compound **3a** shown in Figure 3 appear the most similar to those obtained for riboflavin and can be interpreted based on the mechanism in Scheme 2.³⁹ Compound **3a** (Fl_{ox}) is initially reduced at $E_{\text{f}(1)}^0$ by one-electron to form the radical anion ($\text{Fl}_{\text{rad}}^{\bullet-}$). The radical anion reacts quickly with another flavin by proton transfer to form the neutral radical ($\text{Fl}_{\text{rad}}\text{H}^{\bullet}$) via Eq 1 plus the deprotonated flavin (Fl_{ox}^-). Because $\text{Fl}_{\text{rad}}\text{H}^{\bullet}$ is easier to reduce than Fl_{ox} , it is immediately further reduced at the electrode surface by one-electron to form $\text{Fl}_{\text{red}}\text{H}^-$ at $E_{\text{f}(3)}^0$. Therefore, the first voltammetric process (wave 1) observed at ~ -1.0 V vs. Fc/Fc^+ actually involves two one-electron transfers interspaced with a proton transfer reaction. When the scan direction is reversed at approximately -1.5 V vs. Fc/Fc^+ , two oxidative peaks are observed. The first oxidative peak at ~ -1.0 V vs. Fc/Fc^+ (wave 2) is due to the one-electron oxidation of $\text{Fl}_{\text{rad}}^{\bullet-}$ back to the starting material, Fl_{ox} , while the second oxidative transfer at ~ 0.7 V vs. Fc/Fc^+ is due to the one-electron oxidation of $\text{Fl}_{\text{red}}\text{H}^-$ to $\text{Fl}_{\text{rad}}\text{H}^{\bullet}$ (wave 3). If the equilibrium in Eq 1 in Scheme 2 favours the back reaction (as it does for riboflavin),³⁶ then any $\text{Fl}_{\text{rad}}\text{H}^{\bullet}$ that deprotonates on the voltammetric timescale will also undergo further one-electron oxidation in wave 3 to regenerate the starting material. As the scan rate is increased up to 20 V s^{-1} , the initial reduction process at ~ -1.0 V vs. Fc/Fc^+ becomes more chemically reversible shown by how the $i_{\text{p}}^{\text{ox}}/i_{\text{p}}^{\text{red}}$ ratio approaches unity, due to the proton transfer step between $\text{Fl}_{\text{rad}}^{\bullet-}$ and Fl_{ox} being outrun; hence the reduction process changes to a chemically reversible one-electron transfer.

When the voltammetric scan is extended to more negative potentials, additional reduction processes are detected at ~ -1.7 V vs. Fc/Fc^+ (wave 4) and ~ -2.0 V vs. Fc/Fc^+ (wave 5) for compound **3a**. Wave 4 is associated with the one-electron reduction of Fl_{ox}^- that is formed from the Fl_{ox} reacting with $\text{Fl}_{\text{rad}}^{\bullet-}$ ($E_{\text{f}(4)}^0$), and wave 5 is associated with the further one-electron reduction of $\text{Fl}_{\text{rad}}^{\bullet-}$ to form $\text{Fl}_{\text{red}}^{2-}$ ($E_{\text{f}(5)}^0$). When the forward potential scan is extended all the way past wave 5, on the reverse scan it can be observed that the oxidative wave 3 is larger than when the forward scan is only extended just past wave 1. The reason for wave 3 appearing larger is because $\text{Fl}_{\text{red}}\text{H}^-$ (which undergoes oxidation in wave 3) can also be formed via $\text{Fl}_{\text{red}}^{2-}$ reacting with Fl_{ox} to form $\text{Fl}_{\text{red}}\text{H}^-$ (plus Fl_{ox}^-) (Eq 2).

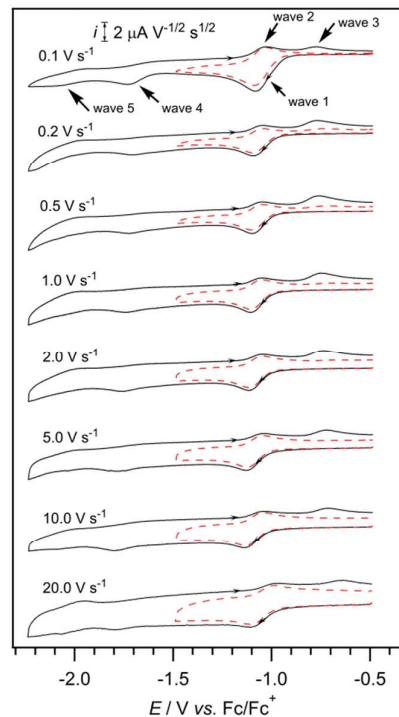


Figure 3. Variable scan rate CVs of 2 mM **3a** in DMSO with 0.2 M $n\text{-Bu}_4\text{NPF}_6$, recorded at a 1 mm Pt electrode at $22 (\pm 2) ^\circ\text{C}$. The current data were scaled by multiplying by $\nu^{-0.5}$.

The voltammetric responses observed for compounds **3b** and **3c** appear somewhat different than **3a**, but they can be interpreted based on exactly the same mechanism as for compound **3a**; the subtle differences in the voltammetric waves can be accounted for by varying equilibrium constants for the homogeneous reactions given in Scheme 2. For example, at relatively slow scan rates the first voltammetric reduction process of **3b** and **3c** appears to be fully chemically reversible implying a simple chemically reversible electron transfer reaction (only wave 1 and 2 are observed), and the process remains chemically reversible as the scan rate is increased up to 20 V s^{-1} . The reason for the high chemical reversibility likely relates to the radical anion ($\text{Fl}_{\text{rad}}^{\bullet-}$) formed in the initial electron transfer step at $E_{\text{f}(1)}^0$ undergoing a slow homogeneous reaction with Fl_{ox} (Eq 1), so on the short voltammetric timescale $\text{Fl}_{\text{rad}}^{\bullet-}$ survives fully at the electrode surface and is able to be converted back to Fl_{ox} when the scan direction is reversed.

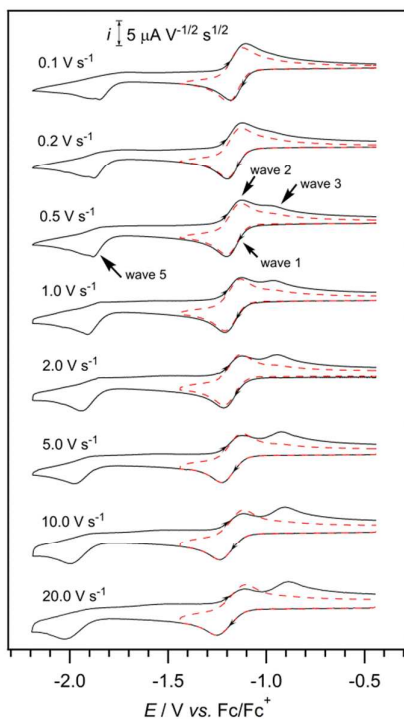


Figure 4. Variable scan rate CVs of 2 mM **3b** in DMSO with 0.2 M *n*-Bu₄NPF₆, recorded at a 1 mm Pt electrode at 22 (±2) °C. The current data were scaled by multiplying by $\nu^{-0.5}$.

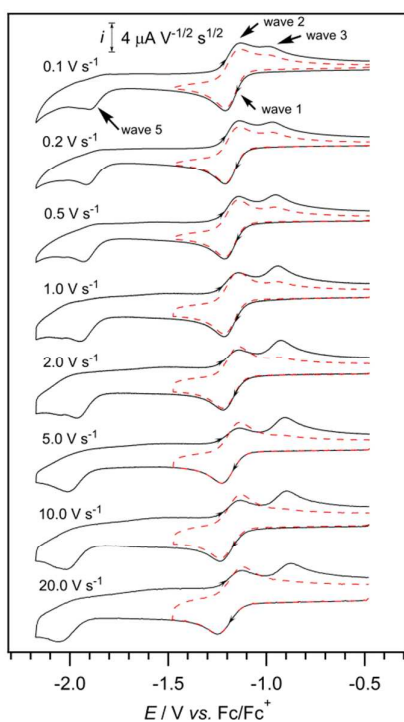


Figure 5. Variable scan rate CVs of 2 mM **3c** in DMSO with 0.2 M *n*-Bu₄NPF₆, recorded at a 1 mm Pt electrode at 22 (±2) °C. The current data were scaled by multiplying by $\nu^{-0.5}$.

When the scan is extended to more negative potentials, compounds **3b** and **3c** show an additional process at ~ -1.8 V vs. Fc/Fc⁺ (wave 5) which, is associated with the further one-electron reduction of Fl_{rad}^{•-} to form Fl_{red}²⁻ ($E_{f(5)}^0$). Wave 5 appears more clearly than was observed during the reduction of compound **3a** because more Fl_{rad}^{•-} exists at the electrode surface in higher amounts (due to the slower proton transfer reaction with Fl_{ox}). Similarly, the reduction process associated with wave 4 ($E_{f(4)}^0$) is not observed during the reduction of **3b** and **3c** because Fl_{ox}⁻ does not have time to form *via* the proton transfer reaction between Fl_{rad}^{•-} and Fl_{ox}. The peak shape of the wave 5 reduction process is "sharp" and this is likely due to some adsorption of the dianion onto the electrode surface. The reason that wave 4 (reduction of Fl_{red}H⁻ to Fl_{red}²⁻) is not observed for compounds **3b** and **3c** may arise either due to a lower acidity of the N-H proton of the starting materials or due to a lowering in basicity of their corresponding anion radicals (Fl_{rad}^{•-}).

When then voltammetric scanning direction was switched at -2.2 V vs. Fc/Fc⁺ after first reducing Fl_{rad}^{•-} to Fl_{red}²⁻, no reverse peak was detected associated with the oxidation of Fl_{red}²⁻ back to Fl_{rad}^{•-} regardless of the scan rate, indicating that the dianion is only very short-lived for compounds **3b** and **3c**. Similarly, when the potential was first scanned to -2.2 V vs. Fc/Fc⁺, on the reverse scan only wave 2 was observed at slow scan rates. However, as the scan rate is increased, wave 3 becomes more pronounced and wave 2 diminishes in size. A reason for this apparently anomalous behaviour can be based on the equilibrium reactions that exist between the different species in Scheme 2 favouring the reformation of Fl_{rad}^{•-}. For example, when the dianion is formed, it immediately undergoes a proton transfer reaction with the starting material to form Fl_{red}H⁻ plus Fl_{ox}⁻ (Scheme 2, Eq 2). Fl_{red}H⁻ then undergoes another reaction with Fl_{ox}⁻ to form two molecules of Fl_{rad}^{•-} (Scheme 2, Eq 3). Therefore, at slow scan rates, Fl_{red}²⁻ has time to convert all the way back to Fl_{rad}^{•-} so only wave 2 is observed, while at faster scan rates, there is only time for Fl_{red}²⁻ to convert to Fl_{red}H⁻ and so wave 3 is mainly observed.

Experimental part

Computational procedures

DFT and TDDFT calculations were performed using Gaussian 09.⁴⁰ For all calculations (geometry optimizations and TDDFT energy calculations), B3LYP^{41,42} was used functional in combination with the 6-31G** basis set.^{43,44} As starting geometry, manually drawn structures were used. For all compounds, the structure was optimized prior to TDDFT energy calculations.

General procedure for the syntheses of compounds **3a-c** (GP1)

A mixture of amine **2a – c** (1 eq), violuric acid **1** (1.2 eq) and 100 mL of glacial acetic acid was added to a round bottom flask and refluxed for 24 h. Acetic acid was removed under reduced pressure, giving a purple solid residue. The residue was purified by flash chromatography on silica gel (chloroform/methanol 50:1) to yield flavin **3a – c** as yellow or red solids.

9-Butylpyreno[4,5-g]pteridine-11,13(9H,12H)-dione (3a)

This compound was synthesized according to **GP1** and after purification by flash chromatography on silica gel (chloroform/methanol 50:1) **3a** (224 mg, 47%) obtained as a red solid. R_f (chloroform/methanol 10:1): 0.44.

M.p. 300 ° (decomp). $^1\text{H-NMR}$ (300 MHz, CF_3COOD , δ ppm): 1.43 (t, $J = 6$ Hz, 3 H), 1.92 (m, 2 H), 2.76 (m, 2 H), 6.19 (t, $J = 6$ Hz, 2 H), 8.76 (m, 4 H), 9.05 (d, $J = 9$ Hz, H), 9.24 (d, $J = 9$ Hz, H), 9.45 (d, $J = 9$ Hz, H), 9.99 (d, $J = 9$ Hz, H). $^{13}\text{C-NMR}$ (300 MHz, CF_3COOD , δ ppm): 11.69 (CH_3), 18.91 (CH_2), 30.47 (CH_2), 59.46 (CH_2), 109.07 (CH), 112.82 (C_{quat}), 116.57 (C_{quat}), 120.32 (CH), 124.93 (CH), 125.64 (CH), 126.94 (CH), 127.45 (CH), 129.21 (C_{quat}), 129.45 (CH), 129.93 (CH), 130.26 (C_{quat}), 132.11 (C_{quat}), 132.36 (C_{quat}), 133.21 (C_{quat}), 136.86 (C_{quat}), 140.18 (C_{quat}), 141.75 (C_{quat}), 144.86 (C_{quat}), 150.12 (C_{quat}). IR (ν , cm^{-1}): 2961 (m), 1652 (s), 1460 (m), 1426 (m), 1400 (m), 1191 (m). UV-Vis (CH_2Cl_2): λ_{max} (ϵ) = 281 (17100), 340 (8480), 355 (8250), 503 (3740), 543 (4370). MS (ES-MS) m/z : 395 (M^+H). MS(HRMS / ESI) m/z : calc. For $\text{C}_{24}\text{H}_{18}\text{N}_4\text{O}_2$ (M^+H): 395.143, found 395.150. Anal. calcd. f. $\text{C}_{24}\text{H}_{18}\text{N}_4\text{O}_2 \cdot 0.5 \text{H}_2\text{O}$: C 71.45, H 4.75, N 13.89, found: C 71.02, H 4.60, N 13.91.

5-Butylanthra[1,2-g]pteridine-1,3(2H,5H)-dione (3b)

The compound was synthesized according to **GP1** and after purification by flash chromatography on silica gel (chloroform/methanol 50:1) **3b** (224 mg, 58 %) obtained as a red solid. R_f (chloroform/methanol 10:1): 0.20.

M.p. 320 ° (decomp). $^1\text{H-NMR}$ (300 MHz, CF_3COOD , δ ppm): 1.69 (t, $J = 6$ Hz, 3 H), 2.36 (m, 2 H), 2.71 (m, 2 H), 5.57 (t, $J = 9$ Hz, 2 H), 8.44 (m, 3 H), 8.85 (dd, $J = 6$ Hz, 2 H), 9.31 (s, H), 9.50 (d, $J = 9$ Hz, H), 10.47 (s, H). $^{13}\text{C-NMR}$ (300 MHz, CF_3COOD , δ ppm): 12.06 (CH_3), 19.36 (CH_2), 29.81 (CH_2), 51.32 (CH_2), 109.06 (CH), 112.81 (C_{quat}), 116.56 (CH), 120.32 (CH), 126.00 (CH), 127.22 (CH), 129.23 (C_{quat}), 129.74 (CH), 129.90 (C_{quat}), 130.49 (C_{quat}), 132.10 (CH), 143.96 (CH), 135.35 (C_{quat}), 136.78 (C_{quat}), 140.06 (C_{quat}), 143.76 (C_{quat}), 150.15 (C_{quat}), 150.49 (C_{quat}). IR (ν , cm^{-1}): 2958 (m), 1647 (s), 1518 (m), 1496 (m), 1448 (m), 1244 (m). UV-Vis (CH_2Cl_2): λ_{max} (ϵ) = 295 (27210), 361 (6900), 505 (5940), 542 (7210). MS (ES-MS) m/z : 371 (M^+H). MS(HRMS / ESI) m/z : calc. For $\text{C}_{22}\text{H}_{18}\text{N}_4\text{O}_2$ (M^+H): 371.1503, found 371.1506.

7-Butylaphto[1,2-g]pteridine-9,11(7H,10H)-dione (3c)³²

The compound was synthesized according to **GP1** and after purification by recrystallization from chloroform **3c** (173 mg, 46 %) was obtained as an orange solid. R_f (chloroform/methanol 10:1): 0.38.

M.p. 280 ° (decomp). $^1\text{H-NMR}$ (300 MHz, CF_3COOD , δ ppm): 1.80 (t, $J = 6$ Hz, 3 H), 2.47 (m, 2 H), 2.82 (m, 2 H), 5.74 (t, $J = 6$ Hz, 2 H), 8.85 (m, 4 H), 9.55 (d, $J = 9$ Hz, H), 10.1 (d, $J = 6$ Hz, H). $^{13}\text{C-NMR}$ (300 MHz, CF_3COOD , δ ppm): 12.16 (CH_3), 19.48 (CH_2), 29.92 (CH_2), 51.41 (CH_2), 109.18 (CH), 112.93 (CH), 116.68 (CH), 120.44 (CH), 125.40 (CH), 129.00 (CH), 130.14 (C_{quat}), 130.65 (C_{quat}), 132.98 (C_{quat}), 133.50 (C_{quat}), 133.70 (C_{quat}), 140.59 (C_{quat}), 141.53 (C_{quat}), 147.61 (C_{quat}). IR (ν , cm^{-1}): 2967 (w), 1638 (s), 1473 (m), 1412 (s), 1202 (m).

UV-Vis (CH_2Cl_2): λ_{max} (ϵ) = 262 (18440), 306 (8170), 315 (8350), 434 (5280), 462 (8210), 490 (7080). MS (ES-MS) m/z : 321 (M^+H). MS(HRMS / ESI) m/z : calc. For $\text{C}_{18}\text{H}_{16}\text{N}_4\text{O}_2$ (M^+H): 321.1273, found 321.1350.

Conclusions

Flavin derivatives **3a-c** were obtained from the condensation of naphthyl-, anthranlyl- or pyrenyl-amines **2a-c** with violuric acid. Extending the π -system of the parent flavin by annulation of a benzene, naphthalene or pyrene unit changes the electronic and redox properties of the chromophore significantly. The chromophore absorption shifts bathochromic and all three compounds show intensive emission with quantum yields of up to 80%. The reduction mechanism of the expanded flavins in DMSO as observed in cyclic voltammetry experiments can be interpreted analogously to the previously investigated parent flavin, with the subtle differences in the voltammetric behaviour due to varying equilibrium constants for the homogeneous reactions following electron transfer.

Acknowledgements

We thank M. Hansen for help with the graphical abstract.

Notes and references

1. J. P. Beardmore, L. M. Antill and J. R. Woodward, *Angew. Chem. Int. Ed.*, 2015, DOI:10.1002/anie.201502591.
2. E. Jortzik, L. Wang, J. Ma and K. Becker, in *Flavins and Flavoproteins*, eds. S. Weber and E. Schleicher, Springer New York, 2014, vol. 1146, ch. 7, pp. 113-157.
3. M. Lee, J. Hong, D.-H. Seo, D. H. Nam, K. T. Nam, K. Kang and C. B. Park, *Angew. Chem. Int. Ed.*, 2013, **52**, 8322-8328.
4. K. S. Conrad, C. C. Manahan and B. R. Crane, *Nat Chem Biol*, 2014, **10**, 801-809.
5. V. Mojz, E. Svobodova, K. Strakova, T. Nevesely, J. Chudoba, H. Dvorakova and R. Cibulka, *Chem. Commun.*, 2015, **51**, 12036-12039.
6. S. K. B. König, R. Cibulka *Chemical Photocatalysis (Ed.: B. König), de Gruyter, Berlin* 2013, 45-66.
7. J. Dařová, S. Kümmel, C. Feldmeier, J. Cibulková, R. Pařout, J. Maixner, R. M. Gschwind, B. König and R. Cibulka, *Chem. Eur. J.*, 2013, **19**, 1066-1075.
8. T. Ghosh, T. Slanina and B. König, *Chem. Sci.*, 2015, **6**, 2027-2034.
9. R. Lechner, S. Kummel and B. König, *Photochem. Photobiol. Sci.*, 2010, **9**, 1367-1377.

10. U. Megerle, M. Wenninger, R.-J. Kutta, R. Lechner, B. Konig, B. Dick and E. Riedle, *Phys. Chem. Chem. Phys.*, 2011, **13**, 8869-8880.
11. B. Muhldorf and R. Wolf, *Chem. Commun.*, 2015, **51**, 8425-8428.
12. D. R. Cardoso, S. H. Libardi and L. H. Skibsted, *Food & Function*, 2012, **3**, 487-502.
13. B. G. Solheim, *Transfusion and Apheresis Science*, 2008, **39**, 75-82.
14. R. Yin, T. Dai, P. Avci, A. E. S. Jorge, W. C. M. A. de Melo, D. Vecchio, Y.-Y. Huang, A. Gupta and M. R. Hamblin, *Current Opin. Pharmacol.*, 2013, **13**, 731-762.
15. J. Glaeser, A. M. Nuss, B. A. Berghoff and G. Klug, in *Advances in Microbial Physiology*, ed. K. P. Robert, Academic Press, 2011, vol. Volume 58, pp. 141-173.
16. M. Insińska-Rak and M. Sikorski, *Chem. Eur. J.*, 2014, **20**, 15280-15291.
17. M. Prongjit, J. Sucharitakul, B. A. Palfey and P. Chaiyen, *Biochemistry*, 2013, **52**, 1437-1445.
18. T. Akiyama, F. Simeno, M. Murakami and F. Yoneda, *J. Am. Chem. Soc.*, 1992, **114**, 6613-6620.
19. B. D. Zoltowski, A. I. Nash and K. H. Gardner, *Biochemistry*, 2011, **50**, 8771-8779.
20. V. Nandwana, I. Samuel, G. Cooke and V. M. Rotello, *Acc. Chem. Res.*, 2013, **46**, 1000-1009.
21. S. Gozem, E. Mirzakulova, I. Schapiro, F. Melaccio, K. D. Glusac and M. Olivucci, *Angew. Chem. Int. Ed.*, 2014, **53**, 9870-9875.
22. M. Szymański, A. Maciejewski and R. P. Steer, *Chem. Phys.*, 1988, **124**, 143-154.
23. S. Sayin, G. Uysal Akkuş, R. Cibulka, I. Stibor and M. Yilmaz, *Helv. Chim. Acta*, 2011, **94**, 481-486.
24. Y.-M. Legrand, M. Gray, G. Cooke and V. M. Rotello, *J. Am. Chem. Soc.*, 2003, **125**, 15789-15795.
25. R. F. Pauszek, G. Kodali, S. T. Caldwell, B. Fitzpatrick, N. Y. Zainalabdeen, G. Cooke, V. M. Rotello and R. J. Stanley, *J. Phys. Chem. B*, 2013, **117**, 15684-15694.
26. F. L. Carter, R. F. Siatkowski and J. Wohltjen, *Molecular Electronic Devices*, Elsevier, Amsterdam, The Netherlands, 1988.
27. J. Jortner and M. A. Ratner, Blackwell, Oxford, 1997.
28. L. Crovetto and S. E. Braslavsky, *The Journal of Physical Chemistry A*, 2006, **110**, 7307-7315.
29. F. Tanaka, H. Chosrowjan, S. Taniguchi, N. Mataga, K. Sato, Y. Nishina and K. Shiga, *J. Phys. Chem. B*, 2007, **111**, 5694-5699.
30. Modified flavins with bathochromic absorption may be of interest for neurobiology. R. H. Kramer, D. L. Fortin and D. Trauner, *Current Opin. Neurobiol.*, 2009, **19**, 544-552.
31. C. M. Marian, S. Nakagawa, V. Rai-Constapel, B. Karasulu and W. Thiel, *J. Phys. Chem. B*, 2014, **118**, 1743-1753.
32. H. Lettre and M.-E. Fernholz, *Berichte der Deutschen Chemischen Gesellschaft B: Abhandlungen*, 1940, 436-441.
33. A. Rosler and W. Pfeleiderer, *Helvetica Chimica Acta*, 1997, **80**, 1869-1881.
34. J. Louie and J. F. Hartwig, *Tetrahedron Lett.*, 1995, **36**, 3609-3612.
35. D. Kumar and K. R. J. Thomas, *J. Photochem. Photobiol. A: Chemistry*, 2011, **218**, 162-173.
36. C. Reichardt, *Angew. Chem. Int. Ed.*, 1979, **18**, 98-110.
37. H. Lettre and M. Fernholz, *Berichte der Deutschen Chemischen Gesellschaft B: Abhandlungen*, 1940, 436.
38. A. Niemz, J. Imbriglio and V. M. Rotello, *J. Am. Chem. Soc.*, 1997, **119**, 887-892.
39. S. L. J. Tan and R. D. Webster, *J. Am. Chem. Soc.*, 2012, **134**, 5954-5964.
40. Gaussian 09, Revision D.01, M. J. Frisch, G. W. Trucks, H. B. Schlegel, G. E. Scuseria, M. A. Robb, J. R. Cheeseman, G. Scalmani, V. Barone, B. Mennucci, G. A. Petersson, H. Nakatsuji, M. Caricato, X. Li, H. P. Hratchian, A. F. Izmaylov, J. Bloino, G. Zheng, J. L. Sonnenberg, M. Hada, M. Ehara, K. Toyota, R. Fukuda, J. Hasegawa, M. Ishida, T. Nakajima, Y. Honda, O. Kitao, H. Nakai, T. Vreven, J. A. Montgomery, Jr., J. E. Peralta, F. Ogliaro, M. Bearpark, J. J. Heyd, E. Brothers, K. N. Kudin, V. N. Staroverov, R. Kobayashi, J. Normand, K. Raghavachari, A. Rendell, J. C. Burant, S. S. Iyengar, J. Tomasi, M. Cossi, N. Rega, J. M. Millam, M. Klene, J. E. Knox, J. B. Cross, V. Bakken, C. Adamo, J. Jaramillo, R. Gomperts, R. E. Stratmann, O. Yazyev, A. J. Austin, R. Cammi, C. Pomelli, J. W. Ochterski, R. L. Martin, K. Morokuma, V. G. Zakrzewski, G. A. Voth, P. Salvador, J. J. Dannenberg, S. Dapprich, A. D. Daniels, Ö. Farkas, J. B. Foresman, J. V. Ortiz, J. Cioslowski, and D. J. Fox, Gaussian, Inc., Wallingford CT, 2009.
41. F. Weigend, R. Ahlrichs, *Phys. Chem. Chem. Phys.*, 2005, **7**, 3297-3305.
42. A. D. Becke, *J. Chem. Phys.*, 1993, **98**, 5648-5652.
43. W. J. Hehre, R. Ditchfield and J. A. Pople, *J. Chem. Phys.* 1972, **56**, 2257-2261.
44. J. D. Dill, J. A. Pople, *J. Chem. Phys.*, 1975, **62**, 2921-2923.